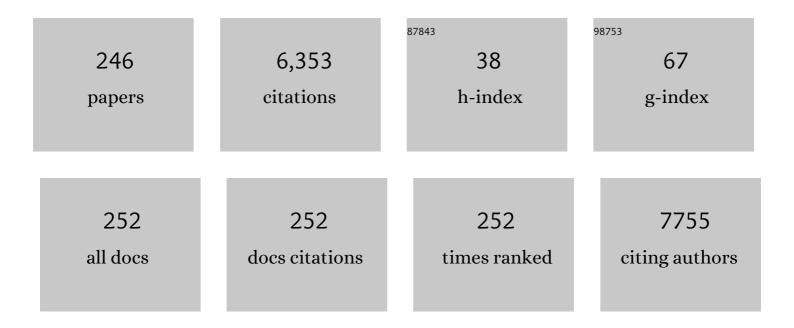
List of Publications by Year in descending order

Source: https://exaly.com/author-pdf/6873965/publications.pdf Version: 2024-02-01



ΜλΙΓΓΓ

#	Article	IF	CITATIONS
1	Improved WATERGATE Pulse Sequences for Solvent Suppression in NMR Spectroscopy. Journal of Magnetic Resonance, 1998, 132, 125-129.	1.2	518
2	Mechanism of Surfactant Micelle Formation. Langmuir, 2008, 24, 10771-10775.	1.6	248
3	Small Infrared Target Detection Based on Weighted Local Difference Measure. IEEE Transactions on Geoscience and Remote Sensing, 2016, 54, 4204-4214.	2.7	226
4	Experimental implementation of remote state preparation by nuclear magnetic resonance. Physics Letters, Section A: General, Atomic and Solid State Physics, 2003, 306, 271-276.	0.9	196
5	Hyperpolarized Xe NMR signal advancement by metal-organic framework entrapment in aqueous solution. Proceedings of the National Academy of Sciences of the United States of America, 2020, 117, 17558-17563.	3.3	175
6	Intermolecular Interaction and the Extended Wormlike Chain Conformation of Chitin in NaOH/Urea Aqueous Solution. Biomacromolecules, 2015, 16, 1410-1417.	2.6	164
7	Infrared small-target detection using multiscale gray difference weighted image entropy. IEEE Transactions on Aerospace and Electronic Systems, 2016, 52, 60-72.	2.6	157
8	High-Resolution Diffusion and Relaxation Edited One- and Two-Dimensional1H NMR Spectroscopy of Biological Fluids. Analytical Chemistry, 1996, 68, 3370-3376.	3.2	145
9	C–I··Â-Ï€ Halogen Bonding Driven Supramolecular Helix of Bilateral <i>N</i> -Amidothioureas Bearing β-Turns. Journal of the American Chemical Society, 2017, 139, 6605-6610.	6.6	101
10	Ultrasensitive MicroRNA Assay via Surface Plasmon Resonance Responses of Au@Ag Nanorods Etching. Analytical Chemistry, 2017, 89, 10585-10591.	3.2	94
11	Mechanism of the Mixed Surfactant Micelle Formation. Journal of Physical Chemistry B, 2010, 114, 7808-7816.	1.2	93
12	Recyclable Universal Solvents for Chitin to Chitosan with Various Degrees of Acetylation and Construction of Robust Hydrogels. ACS Sustainable Chemistry and Engineering, 2017, 5, 2725-2733.	3.2	87
13	Entropy-based window selection for detecting dim and small infrared targets. Pattern Recognition, 2017, 61, 66-77.	5.1	85
14	¹⁹ Fâ€NMR Spectroscopy as a Probe of Cytoplasmic Viscosity and Weak Protein Interactions in Living Cells. Chemistry - A European Journal, 2013, 19, 12705-12710.	1.7	83
15	Measurement of Biomolecular Diffusion Coefficients in Blood Plasma Using Two-Dimensional 1Hâ^'1H Diffusion-Edited Total-Correlation NMR Spectroscopy. Analytical Chemistry, 1997, 69, 1504-1509.	3.2	81
16	Noncovalent Dimerization of Ubiquitin. Angewandte Chemie - International Edition, 2012, 51, 469-472.	7.2	80
17	Solution structure of all parallel G-quadruplex formed by the oncogene RET promoter sequence. Nucleic Acids Research, 2011, 39, 6753-6763.	6.5	71
18	Metabonomic alterations in hippocampus, temporal and prefrontal cortex with age in rats. Neurochemistry International, 2009, 54, 481-487.	1.9	66

#	Article	IF	CITATIONS
19	Metabolic changes in rat prefrontal cortex and hippocampus induced by chronic morphine treatment studied ex vivo by high resolution 1H NMR spectroscopy. Neurochemistry International, 2007, 50, 386-394.	1.9	64
20	The PHD1 finger of KDM5B recognizes unmodified H3K4 during the demethylation of histone H3K4me2/3 by KDM5B. Protein and Cell, 2014, 5, 837-850.	4.8	62
21	Safety analysis of edible oil products via Raman spectroscopy. Talanta, 2019, 191, 324-332.	2.9	56
22	Use of1H NMR-determined diffusion coefficients to characterize lipoprotein fractions in human blood plasma. Magnetic Resonance in Chemistry, 2002, 40, S83-S88.	1.1	55
23	Creating Conformational Entropy by Increasing Interdomain Mobility in Ligand Binding Regulation: A Revisit to N-Terminal Tandem PDZ Domains of PSD-95. Journal of the American Chemical Society, 2009, 131, 787-796.	6.6	53
24	Image enhancement based on intuitionistic fuzzy sets theory. IET Image Processing, 2016, 10, 701-709.	1.4	53
25	Preparation of pseudo-pure states by line-selective pulses in nuclear magnetic resonance. Chemical Physics Letters, 2001, 340, 509-516.	1.2	52
26	G-triplex: A new type of CRISPR-Cas12a reporter enabling highly sensitive nucleic acid detection. Biosensors and Bioelectronics, 2021, 187, 113292.	5.3	52
27	pH-Triggered Au-fluorescent mesoporous silica nanoparticles for ¹⁹ F MR/fluorescent multimodal cancer cellular imaging. Chemical Communications, 2014, 50, 283-285.	2.2	51
28	Structure-guided post-SELEX optimization of an ochratoxin A aptamer. Nucleic Acids Research, 2019, 47, 5963-5972.	6.5	51
29	The intracellular environment affects protein–protein interactions. Proceedings of the National Academy of Sciences of the United States of America, 2021, 118, .	3.3	49
30	Quantification of complementarity in multiqubit systems. Physical Review A, 2005, 72, .	1.0	47
31	Optimization protocol for the extraction of antioxidant components from Origanum vulgare leaves using response surface methodology. Saudi Journal of Biological Sciences, 2016, 23, 389-396.	1.8	47
32	Analysis of Drug–Protein Binding Using Nuclear Magnetic Resonance Based Molecular Diffusion Measurements. Analytical Communications, 1997, 34, 225-228.	2.2	46
33	Solution structure of the Magnaporthe oryzae avirulence protein AvrPiz-t. Journal of Biomolecular NMR, 2013, 55, 219-223.	1.6	46
34	Accurately Probing Slow Motions on Millisecond Timescales with a Robust NMR Relaxation Experiment. Journal of the American Chemical Society, 2008, 130, 2432-2433.	6.6	45
35	Genomic and Structural Characterization of Kunitz-Type Peptide LmKTT-1a Highlights Diversity and Evolution of Scorpion Potassium Channel Toxins. PLoS ONE, 2013, 8, e60201.	1.1	44
36	NMR-Based Methods for Protein Analysis. Analytical Chemistry, 2021, 93, 1866-1879.	3.2	43

#	Article	IF	CITATIONS
37	Conformational Dynamics of apoâ€GInBP Revealed by Experimental and Computational Analysis. Angewandte Chemie - International Edition, 2016, 55, 13990-13994.	7.2	41
38	Macromolecular and Small Molecular Crowding Have Similar Effects on α‧ynuclein Structure. ChemPhysChem, 2017, 18, 55-58.	1.0	41
39	Engineered Paramagnetic Graphene Quantum Dots with Enhanced Relaxivity for Tumor Imaging. Nano Letters, 2019, 19, 441-448.	4.5	41
40	Mitochondria Targeted and Intracellular Biothiol Triggered Hyperpolarized ¹²⁹ Xe Magnetofluorescent Biosensor. Analytical Chemistry, 2017, 89, 2288-2295.	3.2	40
41	CRISPR-Cas12a <i>trans</i> -cleaves DNA G-quadruplexes. Chemical Communications, 2020, 56, 12526-12529.	2.2	40
42	Structural Basis of Molecular Recognition between ESCRT-III-like Protein Vps60 and AAA-ATPase Regulator Vta1 in the Multivesicular Body Pathway. Journal of Biological Chemistry, 2012, 287, 43899-43908.	1.6	39
43	Protein dynamics in living cells studied by inâ€cell NMR spectroscopy. FEBS Letters, 2013, 587, 1008-1011.	1.3	39
44	MRI-visible liposome nanovehicles for potential tumor-targeted delivery of multimodal therapies. Nanoscale, 2015, 7, 12843-12850.	2.8	39
45	A 15N CPMG relaxation dispersion experiment more resistant to resonance offset and pulse imperfection. Journal of Magnetic Resonance, 2015, 257, 1-7.	1.2	39
46	Dissolution and Metastable Solution of Cellulose in NaOH/Thiourea at 8 °C for Construction of Nanofibers. Journal of Physical Chemistry B, 2017, 121, 1793-1801.	1.2	39
47	Direct Observation of Ca ²⁺ â€Induced Calmodulin Conformational Transitions in Intact <i>Xenopus laevis</i> Oocytes by ¹⁹ Fâ€NMR Spectroscopy. Angewandte Chemie - International Edition, 2015, 54, 5328-5330.	7.2	38
48	Delicately Designed Cancer Cell Membrane-Camouflaged Nanoparticles for Targeted ¹⁹ F MR/PA/FL Imaging-Guided Photothermal Therapy. ACS Applied Materials & Interfaces, 2020, 12, 57290-57301.	4.0	38
49	A pH-gated conformational switch regulates the phosphatase activity of bifunctional HisKA-family histidine kinases. Nature Communications, 2017, 8, 2104.	5.8	37
50	MRI-guided liposomes for targeted tandem chemotherapy and therapeutic response prediction. Acta Biomaterialia, 2016, 35, 260-268.	4.1	36
51	Structural Insights into the Mechanism of High-Affinity Binding of Ochratoxin A by a DNA Aptamer. Journal of the American Chemical Society, 2022, 144, 7731-7740.	6.6	36
52	Selective Inverse-Detected Long-Range HeteronuclearJ-Resolved NMR Spectroscopy and Its Application to the Measurement of3JCH. Journal of Magnetic Resonance Series B, 1995, 109, 275-283.	1.6	35
53	Saturation transfer difference nuclear magnetic resonance study on the specific binding of ligand to protein. Analytical Biochemistry, 2009, 385, 380-382.	1.1	35
54	Magnetic Resonance Spectroscopy as a Tool for Assessing Macromolecular Structure and Function in Living Cells. Annual Review of Analytical Chemistry, 2017, 10, 157-182.	2.8	35

#	Article	IF	CITATIONS
55	An evaluation of gadolinium polyoxometalates as possible MRI contrast agent. Magnetic Resonance Imaging, 2002, 20, 407-412.	1.0	34
56	NMR experimental implementation of three-parties quantum superdense coding. Science Bulletin, 2004, 49, 423-426.	1.7	33
57	Optimized Quantitative DEPT and Quantitative POMMIE Experiments for ¹³ C NMR. Analytical Chemistry, 2008, 80, 8293-8298.	3.2	33
58	Impurity profiling in bulk pharmaceutical batches using 19F NMR spectroscopy and distinction between monomeric and dimeric impurities by NMR-based diffusion measurements. Journal of Pharmaceutical and Biomedical Analysis, 1999, 19, 511-517.	1.4	32
59	Comparison between GdDTPA and two gadolinium polyoxometalates as potential MRI contrast agents. Journal of Inorganic Biochemistry, 2002, 92, 193-199.	1.5	32
60	Naked-eye based point-of-care detection of E.coli O157: H7 by a signal-amplified microfluidic aptasensor. Analytica Chimica Acta, 2020, 1130, 20-28.	2.6	32
61	Dynamics of Mixed Surfactants in Aqueous Solutions. Journal of Physical Chemistry B, 2011, 115, 1986-1990.	1.2	31
62	Mammogram Enhancement Using Intuitionistic Fuzzy Sets. IEEE Transactions on Biomedical Engineering, 2017, 64, 1803-1814.	2.5	31
63	Structural basis of DNA binding to human YB-1 cold shock domain regulated by phosphorylation. Nucleic Acids Research, 2020, 48, 9361-9371.	6.5	30
64	1H-NMR study of the effect of acetonitrile on the interaction of ibuprofen with human serum albumin. Journal of Pharmaceutical and Biomedical Analysis, 2002, 30, 151-159.	1.4	29
65	Interaction between calcium-free calmodulin and IQ motif of neurogranin studied by nuclear magnetic resonance spectroscopy. Analytical Biochemistry, 2003, 315, 175-182.	1.1	28
66	Positively Charged Tags Impede Protein Mobility in Cells as Quantified by ¹⁹ F NMR. Journal of Physical Chemistry B, 2019, 123, 4527-4533.	1.2	28
67	Development of a biotinylated nanobody for sensitive detection of aflatoxin B1 in cereal via ELISA. Talanta, 2022, 239, 123125.	2.9	28
68	Concentration-Dependent Aggregation of CHAPS Investigated by NMR Spectroscopy. Journal of Physical Chemistry B, 2010, 114, 3863-3868.	1.2	27
69	Weak interactions and their impact on cellulose dissolution in an alkali/urea aqueous system. Physical Chemistry Chemical Physics, 2017, 19, 17909-17917.	1.3	27
70	Detection and differentiation of Cys, Hcy and GSH mixtures by 19F NMR probe. Talanta, 2018, 184, 513-519.	2.9	27
71	Mass spectrometryâ€based strategies for singleâ€cell metabolomics. Mass Spectrometry Reviews, 2023, 42, 67-94.	2.8	27
72	Compositional differences among Chinese soy sauce types studied by 13C NMR spectroscopy coupled with multivariate statistical analysis. Talanta, 2016, 158, 89-99.	2.9	26

#	Article	IF	CITATIONS
73	pH-responsive theranostic nanocomposites as synergistically enhancing positive and negative magnetic resonance imaging contrast agents. Journal of Nanobiotechnology, 2018, 16, 30.	4.2	26
74	Synthesis and evaluation of novel polysaccharide-Gd-DTPA compounds as contrast agent for MRI. Journal of Magnetism and Magnetic Materials, 2003, 265, 123-129.	1.0	25
75	Functional changes in the frontal cortex in Parkinson's disease using a rat model. Journal of Clinical Neuroscience, 2010, 17, 628-633.	0.8	25
76	Biothiol Xenon MRI Sensor Based on Thiol-Addition Reaction. Analytical Chemistry, 2016, 88, 5835-5840.	3.2	25
77	Increasing Cancer Therapy Efficiency through Targeting and Localized Light Activation. ACS Applied Materials & Interfaces, 2017, 9, 23400-23408.	4.0	25
78	Strategies for Protein NMR in <i>Escherichia coli</i> . Biochemistry, 2014, 53, 1971-1981.	1.2	24
79	An interferometric complementarity experiment in a bulk nuclear magnetic resonance ensemble. Journal of Physics A, 2003, 36, 2555-2563.	1.6	23
80	1H NMR spectroscopic evidence of interaction between ibuprofen and lipoproteins in human blood plasma. Analytical Biochemistry, 2004, 324, 292-297.	1.1	23
81	Labeling Strategy and Signal Broadening Mechanism of Protein NMR Spectroscopy in <i>Xenopus laevis</i> Oocytes. Chemistry - A European Journal, 2015, 21, 8686-8690.	1.7	23
82	Experimental implementation of Hogg's algorithm on a three-quantum-bit NMR quantum computer. Physical Review A, 2002, 65, .	1.0	22
83	Comparison between Gd-DTPA and several bisamide derivatives as potential MRI contrast agents. Bioorganic and Medicinal Chemistry, 2003, 11, 3359-3366.	1.4	22
84	A Molecular Imaging Approach to Mercury Sensing Based on Hyperpolarized ¹²⁹ Xe Molecular Clamp Probe. Chemistry - A European Journal, 2016, 22, 3967-3970.	1.7	22
85	The Study of the Aggregated Pattern of TX100 Micelle by Using Solvent Paramagnetic Relaxation Enhancements. Molecules, 2019, 24, 1649.	1.7	22
86	Structural Basis for Cytochrome c Y67H Mutant to Function as a Peroxidase. PLoS ONE, 2014, 9, e107305.	1.1	22
87	Gridding and fast Fourier transformation on non-uniformly sparse sampled multidimensional NMR data. Journal of Magnetic Resonance, 2010, 204, 165-168.	1.2	21
88	Proton NMR Based Investigation of the Effects of Temperature and NaCl on Micellar Properties of CHAPS. Journal of Physical Chemistry B, 2011, 115, 1991-1998.	1.2	21
89	pH- and concentration-induced micelle-to-vesicle transitions in pyrrolidone-based Gemini surfactants. Colloid and Polymer Science, 2014, 292, 739-747.	1.0	21
90	Ca2+ modulating α-synuclein membrane transient interactions revealed by solution NMR spectroscopy. Biochimica Et Biophysica Acta - Biomembranes, 2014, 1838, 853-858.	1.4	21

#	Article	IF	CITATIONS
91	Quantification of size effect on protein rotational mobility in cells by 19F NMR spectroscopy. Analytical and Bioanalytical Chemistry, 2018, 410, 869-874.	1.9	21
92	Reconstructing diffusion ordered NMR spectroscopy by simultaneous inversion of Laplace transform. Journal of Magnetic Resonance, 2017, 278, 1-7.	1.2	19
93	Crowding and Confinement Can Oppositely Affect Protein Stability. ChemPhysChem, 2018, 19, 3350-3355.	1.0	19
94	Recovery of Underwater Resonances by Magnetization Transferred NMR Spectroscopy (RECUR-NMR). Journal of Magnetic Resonance, 2001, 153, 133-137.	1.2	18
95	NMR Investigation of the Exchange Kinetics of Quaternary Ammonium Dimeric Surfactants C ₁₄ - <i>s</i> -C ₁₄ ·2Br. Journal of Physical Chemistry B, 2008, 112, 2874-2879.	1.2	18
96	1H NMR metabolomics study of metastatic melanoma in C57BL/6J mouse spleen. Metabolomics, 2014, 10, 1129-1144.	1.4	18
97	α-synuclein-lanthanide metal ions interaction: binding sites, conformation and fibrillation. BMC Biophysics, 2015, 9, 1.	4.4	18
98	Influence of cation on the cellulose dissolution investigated by MD simulation and experiments. Cellulose, 2017, 24, 4641-4651.	2.4	18
99	ATP complex of Al3+ as studied by PFG NMR. Spectrochimica Acta - Part A: Molecular and Biomolecular Spectroscopy, 1998, 54, 999-1005.	2.0	17
100	Recent advances in protein NMR spectroscopy and their implications in protein therapeutics research. Analytical and Bioanalytical Chemistry, 2014, 406, 2279-2288.	1.9	17
101	Structural investigation into physiological DNA phosphorothioate modification. Scientific Reports, 2016, 6, 25737.	1.6	17
102	Cation/macromolecule interaction in alkaline cellulose solution characterized with pulsed field-gradient spin-echo NMR spectroscopy. Physical Chemistry Chemical Physics, 2017, 19, 7486-7490.	1.3	17
103	Hyperpolarized ¹²⁹ Xe Magnetic Resonance Imaging Sensor for H ₂ S. Chemistry - A European Journal, 2017, 23, 7648-7652.	1.7	17
104	Determination of the relative NH proton lifetimes of the peptide analogue viomycin in aqueous solution by NMR-based diffusion measurement. Journal of Biomolecular NMR, 1999, 13, 25-30.	1.6	16
105	Dynamic NMR study and theoretical calculations on the conformational exchange of valsartan and related compounds. Magnetic Resonance in Chemistry, 2007, 45, 929-936.	1.1	16
106	Rational design of hyperpolarized xenon NMR molecular sensor for the selective and sensitive determination of zinc ions. Talanta, 2014, 122, 101-105.	2.9	16
107	Simultaneous detection of small molecule thiols with a simple ¹⁹ F NMR platform. Chemical Science, 2021, 12, 1095-1100.	3.7	16
108	Two-dimensional1H1H and13C1H maximum-quantum correlation NMR spectroscopy with application to the assignment of the NMR spectra of the bile salt sodium taurocholate. Magnetic Resonance in Chemistry, 1995, 33, 212-219.	1.1	15

#	Article	IF	CITATIONS
109	1H–14N HSQC detection of choline-containing compounds in solutions. Journal of Magnetic Resonance, 2010, 206, 157-160.	1.2	15
110	NASR: An Effective Approach for Simultaneous Noise and Artifact Suppression in NMR Spectroscopy. Analytical Chemistry, 2013, 85, 2523-2528.	3.2	15
111	13C-NMR-Based Metabolomic Profiling of Typical Asian Soy Sauces. Molecules, 2016, 21, 1168.	1.7	15
112	Enhanced effect of magnetic field gradients using multiple quantum NMR spectroscopy applied to self-diffusion coefficient measurement. Molecular Physics, 1998, 93, 913-920.	0.8	15
113	Multiple quantum correlated spectroscopy revamped by asymmetric z-gradient echo detection signal intensity as a function of the read pulse flip angle as verified by heteronuclear H1â^•P31 experiments. Journal of Chemical Physics, 2007, 126, 054502.	1.2	14
114	Impact of the α-Synuclein Initial Ensemble Structure on Fibrillation Pathways and Kinetics. Journal of Physical Chemistry B, 2016, 120, 3140-3147.	1.2	14
115	Roles of structural plasticity in chaperone HdeA activity are revealed by 19F NMR. Chemical Science, 2016, 7, 2222-2228.	3.7	14
116	Freeâ€base porphyrins as CEST MRI contrast agents with highly upfield shifted labile protons. Magnetic Resonance in Medicine, 2019, 82, 577-585.	1.9	14
117	Double quantum CRAZED NMR signal in inhomogeneous fields. Chemical Physics, 2008, 351, 33-36.	0.9	13
118	Accurately Probing Slow Motions on Millisecond Timescales with a Robust NMR Relaxation Experiment. Journal of the American Chemical Society, 2008, 130, 17629-17629.	6.6	13
119	Body temperature sensitive micelles for MRI enhancement. Chemical Communications, 2015, 51, 9085-9088.	2.2	13
120	Phosphorylation dependent α-synuclein degradation monitored by in-cell NMR. Chemical Communications, 2019, 55, 11215-11218.	2.2	13
121	NMR spectroscopic diffusion, chemical shift and linewidth measurements of low-affinity binding of ibuprofen enantiomers to human serum albumin. Magnetic Resonance in Chemistry, 1999, 37, 269-273.	1.1	12
122	Realization of a Decoherence-Free Subspace Using Multiple Quantum Coherences. Physical Review Letters, 2005, 95, 020501.	2.9	12
123	Constant-variable flip angles for hyperpolarized media MRI. Journal of Magnetic Resonance, 2016, 263, 92-100.	1.2	12
124	Potential detection of cancer with fluorinated silicon nanoparticles in ¹⁹ F MR and fluorescence imaging. Journal of Materials Chemistry B, 2018, 6, 4293-4300.	2.9	12
125	Protein stability analysis in ionic liquids by 19F NMR. Analytical and Bioanalytical Chemistry, 2019, 411, 4929-4935.	1.9	12
126	Measurement of inter-proton distances from cross-relaxation rates determined by a selective null inversion-recovery NMR method. Magnetic Resonance in Chemistry, 1992, 30, 173-176.	1.1	11

#	Article	IF	CITATIONS
127	1H NMR dipolar relaxation times and the derivation of internuclear distance. Concepts in Magnetic Resonance, 1996, 8, 161-173.	1.3	11
128	Diffusion Coefficient Measurement by High Resolution NMR Spectroscopy: Biochemical and Pharmaceutical Applications. Reviews in Analytical Chemistry, 1999, 18, .	1.5	11
129	"Spectral implementation―for creating a labeled pseudo-pure state and the Bernstein–Vazirani algorithm in a four-qubit nuclear magnetic resonance quantum processor. Journal of Chemical Physics, 2004, 120, 3579-3585.	1.2	11
130	A competitive low-affinity binding model for determining the mutual and specific sites of two ligands on protein. Journal of Pharmaceutical and Biomedical Analysis, 2005, 38, 588-593.	1.4	11
131	1H NMR investigation on interaction between ibuprofen and lipoproteins. Chemistry and Physics of Lipids, 2007, 148, 105-111.	1.5	11
132	The impact of pulse duration on composite WATERGATE pulse. Journal of Magnetic Resonance, 2010, 206, 205-209.	1.2	11
133	Dominant Conformation of Valsartan in Sodium Dodecyl Sulfate Micelle Environment. Journal of Physical Chemistry B, 2010, 114, 2719-2727.	1.2	11
134	Structural Basis for the Inhibition of the Autophosphorylation Activity of HK853 by Luteolin. Molecules, 2019, 24, 933.	1.7	11
135	A Small Molecular Multifunctional Tool for pH Detection, Fluorescence Imaging, and Photodynamic Therapy. ACS Applied Bio Materials, 2020, 3, 1779-1786.	2.3	11
136	A virtual-droplet system for sensing MMP9 activity of single suspended and adhered cancer cells. Sensors and Actuators B: Chemical, 2020, 308, 127749.	4.0	11
137	A Selective NMR Method for Detecting Choline Containing Compounds in Liver Tissue: The ¹ Hâ^' ¹⁴ N HSQC Experiment. Journal of the American Chemical Society, 2010, 132, 17349-17351.	6.6	10
138	Confinement Alters the Structure and Function of Calmodulin. Angewandte Chemie - International Edition, 2017, 56, 530-534.	7.2	10
139	Uncorrelated Effect of Interdomain Contact on Pin1 Isomerase Activity Reveals Positive Catalytic Cooperativity. Journal of Physical Chemistry Letters, 2019, 10, 1272-1278.	2.1	10
140	Chaperone Spy Protects Outer Membrane Proteins from Folding Stress via Dynamic Complex Formation. MBio, 2021, 12, e0213021.	1.8	10
141	Three-Dimensional Maximum-Quantum Correlation HMQC NMR Spectroscopy (3D MAXY-HMQC). Journal of Magnetic Resonance, 1997, 129, 67-73.	1.2	9
142	Multiple-Quantum J-Resolved NMR Spectroscopy (MQ-JRES): Measurement of Multiple-Quantum Relaxation Rates and Relative Signs of Spin Coupling Constants. Journal of Magnetic Resonance, 2000, 146, 277-282.	1.2	9
143	Implementation of real-time two-dimensional nuclear magnetic resonance spectroscopy for on-flow high-performance liquid chromatography. Journal of Chromatography A, 2007, 1154, 464-468.	1.8	9
144	Understanding the Interaction between Valsartan and Detergents by NMR Techniques and Molecular Dynamics Simulation. Journal of Physical Chemistry B, 2012, 116, 7470-7478.	1.2	9

#	Article	IF	CITATIONS
145	Measurement of amide proton chemical shift anisotropy in perdeuterated proteins using CSA amplification. Journal of Magnetic Resonance, 2017, 284, 33-38.	1.2	9
146	Calcium accelerates SNARE-mediated lipid mixing through modulating α-synuclein membrane interaction. Biochimica Et Biophysica Acta - Biomembranes, 2018, 1860, 1848-1853.	1.4	9
147	Conformational Toggling of Yeast Iso-1-Cytochrome c in the Oxidized and Reduced States. PLoS ONE, 2011, 6, e27219.	1.1	9
148	NMR structures of fusion peptide from influenza hemagglutinin H3 subtype and its mutants. Journal of Peptide Science, 2014, 20, 292-297.	0.8	8
149	An intracellular diamine oxidase triggered hyperpolarized ¹²⁹ Xe magnetic resonance biosensor. Chemical Communications, 2018, 54, 13654-13657.	2.2	8
150	Membraneâ€mediated disorderâ€toâ€order transition of SNAP25 flexible linker facilitates its interaction with syntaxinâ€1 and SNAREâ€complex assembly. FASEB Journal, 2019, 33, 7985-7994.	0.2	8
151	Enhancing the detection sensitivity of nanobody against aflatoxin B1 through structure-guided modification. International Journal of Biological Macromolecules, 2022, 194, 188-197.	3.6	8
152	The first application of the Vogel–Fulcher–Tammann equation to biological problem: A new interpretation of the temperature dependent hydrogen exchange rates of the thrombin-binding DNA. Physics Letters, Section A: General, Atomic and Solid State Physics, 2007, 361, 248-251.	0.9	7
153	Metabolic changes in temporal lobe structures measured by HR-MAS NMR at early stage of electrogenic rat epilepsy. Experimental Neurology, 2008, 212, 377-385.	2.0	7
154	Conformational and dynamics simulation study of antimicrobial peptide hedistin—heterogeneity of its helix–turn–helix motif. Biochimica Et Biophysica Acta - Biomembranes, 2009, 1788, 2497-2508.	1.4	7
155	Fast detection of choline-containing metabolites in liver using 2D 1H–14N three-bond correlation (HN3BC) spectroscopy. Journal of Magnetic Resonance, 2012, 214, 352-359.	1.2	7
156	NMR Spectroscopic Approach Reveals Metabolic Diversity of Human Blood Plasma Associated with Protein–Drug Interaction. Analytical Chemistry, 2013, 85, 8601-8608.	3.2	7
157	A peripheral component interconnect express-based scalable and highly integrated pulsed spectrometer for solution state dynamic nuclear polarization. Review of Scientific Instruments, 2015, 86, 083101.	0.6	7
158	Structural insights into the impact of two holoprosencephaly-related mutations on human TGIF1 homeodomain. Biochemical and Biophysical Research Communications, 2018, 496, 575-581.	1.0	7
159	Structure of membrane diacylglycerol kinase in lipid bilayers. Communications Biology, 2021, 4, 282.	2.0	7
160	NMR experimental realization of seven-qubit D-J algorithm and controlled phase-shift gates with improved precision. Science Bulletin, 2003, 48, 239-243.	1.7	6
161	Structure-based drug design: NMR-based approach for ligand–protein interactions. Drug Discovery Today: Technologies, 2006, 3, 241-245.	4.0	6
162	NMRâ€based Metabonomic Study on Rat's Urinary Metabolic Response to Dosage of Triptolide. Chinese Journal of Chemistry, 2009, 27, 751-758.	2.6	6

#	Article	IF	CITATIONS
163	Protein dynamics elucidated by NMR technique. Protein and Cell, 2013, 4, 726-730.	4.8	6
164	Characterizing oils in oil-water mixtures inside porous media by Overhauser dynamic nuclear polarization. Fuel, 2019, 257, 116107.	3.4	6
165	REALâ€ <i>t</i> ₁ , an Effective Approach for <i>t</i> ₁ â€Noise Suppression in NMR Spectroscopy Based on Resampling Algorithm. Chinese Journal of Chemistry, 2020, 38, 77-81.	2.6	6
166	NMR Reveals the Conformational Changes of Cytochrome C upon Interaction with Cardiolipin. Life, 2021, 11, 1031.	1.1	6
167	Comparison of Maximum Quantum Filtered NMR Spectroscopy (MAXY NMR) and Other Two-Dimensional NMR Approaches for Resonance Assignment of Peptides. , 1996, 34, 865-872.		5
168	Eliminating systematic error in multiple quantum diffusion measurements by bipolar gradient pulses. Measurement Science and Technology, 1998, 9, 1347-1350.	1.4	5
169	Improved one-dimensional NMR detection of heteronuclear multiple quantum coherence involving the insensitive nucleus as demonstrated by the compound. Measurement Science and Technology, 1999, 10, 170-173.	1.4	5
170	Mutagenesis and Nuclear Magnetic Resonance Analyses of the Fusion Peptide of <i>Helicoverpa armigera</i> Single Nucleocapsid Nucleopolyhedrovirus F Protein. Journal of Virology, 2008, 82, 8138-8148.	1.5	5
171	Isomeric Effect on H/D Exchange of Resveratrol Studied by NMR Spectroscopy. Chinese Journal of Chemistry, 2010, 28, 2281-2286.	2.6	5
172	Biomolecular ligands screening using radiation damping difference WaterLOGSY spectroscopy. Journal of Biomolecular NMR, 2013, 56, 285-290.	1.6	5
173	Conformational Dynamics of apoâ€ClnBP Revealed by Experimental and Computational Analysis. Angewandte Chemie, 2016, 128, 14196-14200.	1.6	5
174	Characterization and Comparison of Commercial Chinese Cereal and European Grape Vinegars Using ¹ H NMR Spectroscopy Combined with Multivariate Analysis. Chinese Journal of Chemistry, 2016, 34, 1183-1193.	2.6	5
175	The Effects of Macromolecular Crowding on Calmodulin Structure and Function. Chemistry - A European Journal, 2017, 23, 6736-6740.	1.7	5
176	Confinement Alters the Structure and Function of Calmodulin. Angewandte Chemie, 2017, 129, 545-549.	1.6	5
177	Solution structure of SHIP2 SH2 domain and its interaction with a phosphotyrosine peptide from c-MET. Archives of Biochemistry and Biophysics, 2018, 656, 31-37.	1.4	5
178	Expression, purification and characterization of the RhoA-binding domain of human SHIP2 in E.coli. Protein Expression and Purification, 2021, 180, 105821.	0.6	5
179	NMR for Mixture Analysis: Concentration-Ordered Spectroscopy. Analytical Chemistry, 2021, 93, 9697-9703.	3.2	5
180	Structural Insight into the Binding of TGIF1 to SIN3A PAH2 Domain through a C-Terminal Amphipathic Helix. International Journal of Molecular Sciences, 2021, 22, 12631.	1.8	5

#	Article	IF	CITATIONS
181	A fast microfluidic mixer enabling rapid preparation of homogeneous PEG and bicelle media for RDC in NMR analysis. Chemical Engineering Journal, 2022, 431, 133817.	6.6	5
182	Quantum computation based on magic-angle-spinning solid state nuclear magnetic resonance spectroscopy. European Physical Journal B, 2001, 24, 23-35.	0.6	4
183	Quantitative Estimation of Property Parameters of Crude Oil Using Two-Dimensional 13C–1H J-resolved Nuclear Magnetic Resonance Spectroscopy (HET-JRES). Applied Spectroscopy, 2003, 57, 1190-1195.	1.2	4
184	High-resolution magic-angle spinning13C spectroscopy of brain tissue at natural abundance. Magnetic Resonance in Chemistry, 2006, 44, 263-268.	1.1	4
185	Quantitative estimation of SPINOE enhancement in solid state. Journal of Magnetic Resonance, 2009, 196, 200-203.	1.2	4
186	Beryllium Fluoride Exchange Rate Accelerated by Mg ²⁺ as Discovered by ¹⁹ F NMR. Journal of Physical Chemistry A, 2015, 119, 24-28.	1.1	4
187	Simultaneous acquisition of multi-nuclei enhanced NMR/MRI by solution-state dynamic nuclear polarization. Science China Chemistry, 2016, 59, 830-835.	4.2	4
188	Solution NMR structure of RHE_CH02687 from <i>Rhizobium etli</i> : A novel flavonoid-binding protein. Proteins: Structure, Function and Bioinformatics, 2017, 85, 951-956.	1.5	4
189	Solution NMR structure of zinc finger 4 and 5 from human INSM1, an essential regulator of neuroendocrine differentiation. Proteins: Structure, Function and Bioinformatics, 2017, 85, 957-962.	1.5	4
190	Structural insight into the length-dependent binding of ssDNA by SP_0782 from Streptococcus pneumoniae, reveals a divergence in the DNA-binding interface of PC4-like proteins. Nucleic Acids Research, 2019, 48, 432-444.	6.5	4
191	Quantitative Proteomic Analysis for High- and Low-Aflatoxin-Yield Aspergillus flavus Strains Isolated From Natural Environments. Frontiers in Microbiology, 2021, 12, 741875.	1.5	4
192	Recent Advances in Editing and Selective Detection Methods for 1 H NMR Spectroscopy. Current Organic Chemistry, 2001, 5, 351-371.	0.9	4
193	Fast nuclear magnetic resonance correlation spectroscopy without diagonal peaks: The "2-1― correlation spectroscopy. Review of Scientific Instruments, 2008, 79, 026104.	0.6	3
194	1H, 13C and 15N resonance assignments of the N-terminal domain of Vta1–Vps60 peptide complex. Biomolecular NMR Assignments, 2013, 7, 331-334.	0.4	3
195	Impact of Magnesium(II) on Beryllium Fluorides in Solutions Studied by ¹⁹ F NMR Spectroscopy. Chinese Journal of Chemistry, 2014, 32, 878-882.	2.6	3
196	NMR Based Cerebrum Metabonomic Analysis Reveals Simultaneous Interconnected Changes during Chick Embryo Incubation. PLoS ONE, 2015, 10, e0139948.	1.1	3
197	A europium–lipoprotein nanocomposite for highly-sensitive MR-fluorescence multimodal imaging. RSC Advances, 2015, 5, 1808-1811.	1.7	3
198	NMR studies on the interactions between yeast Vta1 and Did2 during the multivesicular bodies sorting pathway. Scientific Reports, 2016, 6, 38710.	1.6	3

#	Article	IF	CITATIONS
199	Dimerization and Conformational Exchanges of the Receiver Domain of Response Regulator PhoB from <i>Escherichia coli</i> . Journal of Physical Chemistry B, 2018, 122, 5749-5757.	1.2	3
200	Chemical shift assignments of a camelid nanobody against aflatoxin B1. Biomolecular NMR Assignments, 2019, 13, 75-78.	0.4	3
201	An untargeted 13C isotopic evaluation approach for the discrimination of fermented food matrices at natural abundance: Application to vinegar. Talanta, 2020, 210, 120679.	2.9	3
202	05SAR-PAGE: Separation of protein dimerization and modification using a gel with 0.05% sarkosyl. Analytica Chimica Acta, 2020, 1101, 193-198.	2.6	3
203	Rational modulation of the enzymatic intermediates for tuning the phosphatase activity of histidine kinase HK853. Biochemical and Biophysical Research Communications, 2020, 523, 733-738.	1.0	3
204	An auxiliary binding interface of SHIP2-SH2 for Y292-phosphorylated FcγRIIB reveals diverse recognition mechanisms for tyrosine-phosphorylated receptors involved in different cell signaling pathways. Analytical and Bioanalytical Chemistry, 2022, 414, 497-506.	1.9	3
205	Structural Investigations on the SH3b Domains of Clostridium perfringens Autolysin through NMR Spectroscopy and Structure Simulation Enlighten the Cell Wall Binding Function. Molecules, 2021, 26, 5716.	1.7	3
206	Self-Assembled Oligopeptide (FK) ₄ as a Chiral Alignment Medium for the Anisotropic NMR Analysis of Organic Compounds. ACS Applied Materials & Interfaces, 2022, 14, 29223-29229.	4.0	3
207	Non-equilibrium crystallization-aggregation mechanism of a-C:H layer in a-C:H/a-Se complex films. Journal of Materials Science Letters, 1990, 9, 1371-1375.	0.5	2
208	Studies of tautomerism and protonation in 2-aryl-1H-imidazo[1,2-a]imidazole derivatives using1H and13C NMR. Magnetic Resonance in Chemistry, 1991, 29, 1147-1151.	1.1	2
209	Parkinson's disease: <i>in vivo</i> metabolic changes in the frontal and parietal cortices in 6-OHDA treated rats during different periods. International Journal of Neuroscience, 2014, 124, 125-132.	0.8	2
210	Chemical shift assignments of the homodimer protein SP_0782 (7–79) from Streptococcus pneumoniae. Biomolecular NMR Assignments, 2016, 10, 341-344.	0.4	2
211	Chemical shift assignments of polyketide cyclase_like protein CGL2373 from Corynebacterium glutamicum. Biomolecular NMR Assignments, 2017, 11, 289-292.	0.4	2
212	Backbone resonance assignment of the response regulator protein PhoBNF20D from Escherichia coli. Biomolecular NMR Assignments, 2018, 12, 133-137.	0.4	2
213	Monitoring alkaline transitions of yeast iso-1 cytochrome c at natural isotopic abundance using trimethyllysine as a native NMR probe. Chemical Communications, 2018, 54, 12630-12633.	2.2	2
214	Characterization of the aggregated pattern of CHAPS using solvent paramagnetic relaxation enhancements. Colloids and Surfaces A: Physicochemical and Engineering Aspects, 2018, 555, 332-338.	2.3	2
215	Characterization of the interaction interface and conformational dynamics of human TGIF1 homeodomain upon the binding of consensus DNA. Biochimica Et Biophysica Acta - Proteins and Proteomics, 2018, 1866, 1021-1028.	1.1	2
216	Chemical shift assignments of the catalytic and ATP-binding domain of HK853 from Thermotoga maritime. Biomolecular NMR Assignments, 2019, 13, 173-176.	0.4	2

#	Article	IF	CITATIONS
217	CSI-LSTM: a web server to predict protein secondary structure using bidirectional long short term memory and NMR chemical shifts. Journal of Biomolecular NMR, 2021, 75, 393-400.	1.6	2
218	Molecular Insight into the Extracellular Chaperone Serum Albumin in Modifying the Folding Free Energy Landscape of Client Proteins. Journal of Physical Chemistry Letters, 2022, 13, 2711-2717.	2.1	2
219	Lanmodulin remains unfolded and fails to interact with lanthanide ions in <i>Escherichia coli</i> cells. Chemical Communications, 2022, 58, 8230-8233.	2.2	2
220	Telomere G-triplex lights up Thioflavin T for RNA detection: new wine in an old bottle. Analytical and Bioanalytical Chemistry, 2022, 414, 6149-6156.	1.9	2
221	Three-qubit quantum error-correction scheme based on quantum cloning. Physics Letters, Section A: General, Atomic and Solid State Physics, 2004, 329, 294-297.	0.9	1
222	Probing single protein with electron spin resonance in combination with shallow nitrogen vacancy. Science China Chemistry, 2015, 58, 833-833.	4.2	1
223	Tracing the micro-process of co-aggregation between binary surfactants in aqueous solutions using 1H NMR. Colloids and Surfaces A: Physicochemical and Engineering Aspects, 2018, 550, 132-137.	2.3	1
224	Chemical shift assignments of CHU_1110: an AHSA1-like protein from Cytophaga hutchinsonii. Biomolecular NMR Assignments, 2018, 12, 155-158.	0.4	1
225	Chemical shift assignments of RHE_RS02845, a NTF2-like domain-containing protein from Rhizobium etli. Biomolecular NMR Assignments, 2018, 12, 249-252.	0.4	1
226	Backbone and side chain resonance assignments of the C-terminal domain of human TGIF1. Biomolecular NMR Assignments, 2019, 13, 357-360.	0.4	1
227	Solution NMR structure of CHU_1110 from <i>Cytophaga hutchinsonii</i> , an AHSA1 protein potentially involved in metal ion stress response. Proteins: Structure, Function and Bioinformatics, 2019, 87, 91-95.	1.5	1
228	Solution NMR structure of CGL2373, a polyketide cyclaseâ€like protein from Corynebacterium glutamicum. Proteins: Structure, Function and Bioinformatics, 2020, 88, 237-241.	1.5	1
229	Accurate estimation of diffusion coefficient for molecular identification in a complex background. Analytical and Bioanalytical Chemistry, 2020, 412, 4519-4525.	1.9	1
230	Mutation of leucine 20 causes a change of local conformation indirectly impairing the DNA binding of SP_0782 from Streptococcus pneumoniae. Biochemical and Biophysical Research Communications, 2020, 524, 103-108.	1.0	1
231	THz-enhanced dynamic nuclear polarized liquid spectrometer. Journal of Magnetic Resonance, 2021, 330, 107044.	1.2	1
232	Bonding and nonequilibrium crystallization of a-C:H/a-Se and a-C:H/KCl. , 1991, 1362, 696.		0
233	Configuration and crystallization ofa-Câ^¶H Film on Ge and Si substrates. Journal of Materials Science, 1993, 28, 5313-5316.	1.7	0
234	Measurement of longitudinal relaxation times in crowded1H NMR spectra using one- and two-dimensional maximum quantum (MAXY) NMR spectroscopy. Molecular Physics, 2001, 99, 1701-1707.	0.8	0

#	Article	IF	CITATIONS
235	Responses of multiple quantum coherences to a double resonant irradiation. Journal of Molecular Structure, 2002, 602-603, 335-345.	1.8	0
236	1H–31P Soft-HSQC Pulse Sequence Specifically for Detecting Phosphomono- and Diesters in Biological Samples. Molecular Imaging and Biology, 2013, 15, 245-249.	1.3	0
237	Frontispiece: Labeling Strategy and Signal Broadening Mechanism of Protein NMR Spectroscopy inXenopus laevisOocytes. Chemistry - A European Journal, 2015, 21, n/a-n/a.	1.7	0
238	New researches of State Key Laboratories in Analytical Chemistry. Science China Chemistry, 2016, 59, 781-782.	4.2	0
239	Chemical shift assignments of Mb1858 (24-155), a FHA domain-containing protein from Mycobacterium bovis. Biomolecular NMR Assignments, 2018, 12, 1-4.	0.4	0
240	Determining the number of chemical species in nuclear magnetic resonance data matrix by taking advantage of collinearity and noise. Analytica Chimica Acta, 2018, 1022, 20-27.	2.6	0
241	Solution NMR structure and ligand identification of human Gas7 SH3 domain reveal a typical SH3 fold but a non-canonical ligand-binding mode. Biochemical and Biophysical Research Communications, 2019, 516, 1190-1195.	1.0	0
242	Mechanisms of Chaperones as Active Assistant/Protector for Proteins: Insights from NMR Studies. Chinese Journal of Chemistry, 2020, 38, 406-413.	2.6	0
243	â^'22-Fold of 1H signal enhancement in-situ low-field liquid NMR using nanodiamond as polarizer of overhauser dynamic nuclear polarization. Chinese Chemical Letters, 2021, 32, 3483-3486.	4.8	0
244	Recent Progress in the Nuclear Magnetic Resonance Applications in Analytical Chemistry. Acta Chimica Sinica, 2012, 70, 2005.	0.5	0
245	Biosensors for single-cell proteomic characterization. , 2022, , 7-36.		0
246	Recent progress in structural study of DNA and its protein and small molecule complexes through NMR spectroscopy. Scientia Sinica Chimica, 2022, , .	0.2	0